ANAYSIS OF LUBRICANT BEHAVIOUR AND ROLL DEFORMATION DURING COLD ROLLING OF STEEL

T.G. Myers * and J.P.F. Charpin†

Workshop participants:

Jon Chapman, Jean Charpin, Mubanga Lombe, Raseelo Moitsheki, Peter Mhone, Tim Myers, Chris Breward

Abstract

In this report we describe a series of basic models for the fluid and solid behaviour during the cold rolling process. We first carry out a simple order of magnitude analysis to determine that the lubricant viscosity varies primarily due to the high pressure in the contact whilst the temperature induced variation is small. We then investigate isoviscous flow under a rigid roller. This results in film thickness predictions below typical surface roughness values. Incorporating the effect of viscosity variation leads to film thicknesses approximately twice those of the isoviscous theory. However, this is still on the order of surface roughness scales. The flow analysis indicates that solid deformation must also be modelled, hence, in the final section we investigate the effect of plastic deformation. Using standard techniques we produce typical pressure profiles within the deformed region. These show that the pressure can exceed the yield stress, and it increases with decreasing strip thickness.

1 Introduction

During the cold rolling process a metal strip is passed between two large rollers. High contact pressure is maintained in order to reduce the thickness

*School of Mathematics and Applied Mathematics, University of Cape Town, Private Bag, Rondebosch 7701. *e-mail: myers@maths.uct.ac.za*

†School of Mathematics and Applied Mathematics, University of Cape Town, Private Bag, Rondebosch 7701. *e-mail: jcharpin@maths.uct.ac.za*

of the strip. Since the process is continuous a basic mass balance shows that the deformed strip must emerge at a higher velocity than when it enters the work zone. Obviously, the rollers move at a constant velocity, which must therefore differ from that of the strip almost everywhere within the gap. For this reason a lubricant is introduced to permit slip.

The following report details an investigation of certain aspects of this process. We focus mainly on the lubricant flow. As detailed in the original problem description, the type and flow rate of the oil used during the cold rolling of stainless steel controls both the friction and heat removal, and thus the surface quality (especially brightness) of the final product. Surface roughness also plays an important role. Columbus Stainless Steel asked the group to investigate the flow of lubricant and roll deformation to enable better control on the important variables.

We start by looking at the lubricant, to estimate its likely behaviour under typical operating conditions. We then look at the flow under rigid rollers and show that it is necessary to introduce the effect of pressure on viscosity. Finally we move on to the plastic deformation and present a simple analysis to determine the pressure, load and moment within the plastic work zone. In the conclusion we discuss numerous effects that could/should be considered given more time and resources.

The process configuration is depicted in Figure 1. The metal strip of thickness $2t_i$ moves towards the rotating rollers at velocity v_i. At some point $x = x_i$ significant plastic deformation occurs. The strip then conforms approximately to the roller shape and emerges at the minimum thickness $2t_o$. Note, some authors introduce a small region of elastic deformation prior to the plastic region, see [7] for example. However, Johnson [4] points out that the elastic deformation is significantly smaller than the plastic deformation and may be neglected at leading order. This simplified approach has proved popular, see [6, 9] for example. To reduce friction and improve the quality of the final product a lubricant is fed between the steel and rollers.

2 Lubricant behaviour in the nip

Lubricant viscosity, subject to pressure and temperature variation, is well-known to follow the modified Barus law

$$\eta = \eta_0 e^{\alpha(p-p_0)-\beta(T-T_0)} \qquad (1)$$

where η_0 is the reference viscosity, α and β indicate the effect that pressure and temperature have on the fluid and p_0, T_0 are the reference pressure and

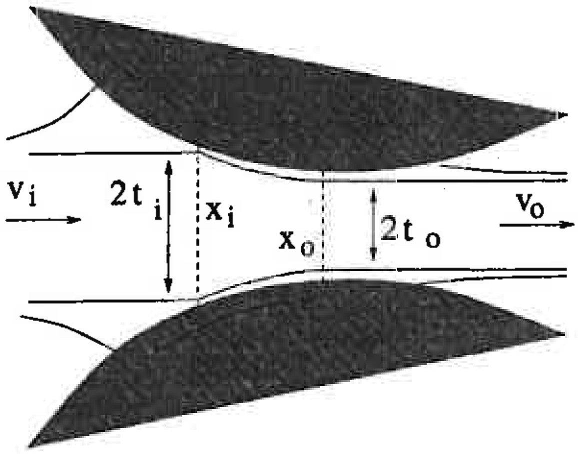

Figure 1: Schematic of roller and typical pressure profile

temperature (when $p = p_0$, $T = T_0$ then $\eta = \eta_0$).

For α and β we choose values typical for a mineral oil, $\alpha = 2 \times 10^{-8}$ Pa^{-1}, $\beta = 0.04°C^{-1}$. We know that the local pressure will not exceed the yield stress, since this results in plastic flow of the solid which then spreads the load more evenly, hence the maximum pressure within the gap is $p_m = \sigma_Y \sim 200$MPa. Finally, from the observations of Columbus Stainless Steel we know that the temperature rise is low, possibly up to 10°C. During the meeting a numerical model for the coupled flow and thermal behaviour was analysed. This confirmed the small temperature rise.

We are now in a position to estimate the viscosity change through the contact region. If we assume p_0 to be the ambient pressure then this is negligible compared to p_m. So, the effect of pressure gives

$$\frac{\eta}{\eta_0} = e^{\alpha p_m} \sim 55 \ ,$$

the effect of the temperature variation gives

$$\frac{\eta}{\eta_0} = e^{-\beta(T-T_0)} \sim 0.67 \ .$$

From this analysis we can see that the very high pressures involved in the flow act to increase the viscosity by a factor of 55. The temperature does act to reduce the viscosity slightly, however, it is clear that the main effect on the flow is pressure and so, if we wish to accurately model the flow and deformation, we should include this effect in our analysis.

In the following section we investigate the pressure distribution under a rigid roller, to gain insight into the typical film thicknesses and pressures experienced by the fluid. Initially we start with an isoviscous fluid, to demonstrate the mathematical method clearly. However, as we have just shown, the pressure has a significant effect on the viscosity and so we subsequently move on to the piezoviscous problem.

3 Pressure distribution under a rigid roller

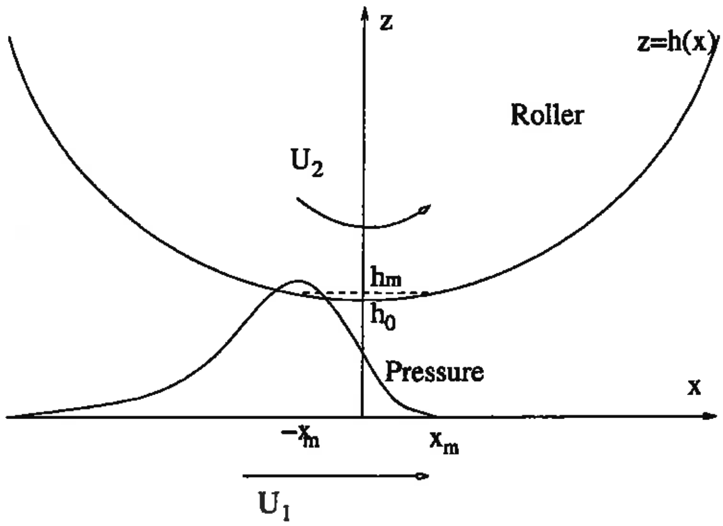

Figure 2: Schematic of roller and typical pressure profile

The problem configuration is shown on Figure 2. We consider a rigid roller and rigid substrate and so, initially, consider just the lubricant behaviour. The roller, defined by $z = h(x)$, lies above a flat surface, which represents the steel sheet. The velocity at the roller circumference is U_2, the surface moves at velocity U_1. The standard form for the pressure is also plotted, indicating that the pressure is small far behind the roller, $x \rightarrow -\infty$, and increases to a maximum at an, as yet, unknown position $(-x_m, h_m)$. It subsequently decreases to zero at (x_m, h_m). The reason that the pressure is zero at x_m will be made clear subsequently or see [1] for example. Obviously the roller cross-section is circular, however, since the nip region is considerably smaller than the cylinder radius (see the results in §3.3) it is well approximated in this region by a quadratic

$$h = h_0 + \frac{x^2}{2R} , \tag{2}$$

where R is the roller radius. This approximation is widely used and known to be accurate for most engineering applications, [2], [4, p322].

The fluid flow is described by the standard lubrication approximation to the Navier-Stokes equations

$$-\frac{\partial p}{\partial x} + \frac{\partial}{\partial z}\left(\eta \frac{\partial u}{\partial z}\right) = 0 \,, \qquad \frac{\partial p}{\partial z} = 0 \,,$$

where u is the fluid velocity in the x direction and p is the fluid pressure. The second equation tells us that the pressure varies only in the x-direction. As shown in the previous section the viscosity $\eta \approx \eta_0 \exp(\alpha p)$, hence $\eta = \eta(x)$. We may therefore integrate the first equation with respect to z immediately. Applying no-slip boundary conditions on $z = 0, h$ we find

$$u = \frac{p_x}{2\eta}(z^2 - hz) + \frac{(U_2 - U_1)}{h} z + U_1 \,. \tag{3}$$

Integrating across the film we obtain an expression for the flux of fluid through the gap

$$Q = \frac{h}{12\eta}\left[6\eta(U_1 + U_2) - p_x h^2\right] \,. \tag{4}$$

Rearranging this leads to the standard Reynolds equation which expresses the pressure gradient in terms of the flux. We may express this in a familiar form

$$\frac{\partial p}{\partial x} = \frac{6\eta(U_1 + U_2)(h - h_m)}{h^3} \,, \tag{5}$$

where h_m is the unknown height at which the pressure gradient is zero. Since the cylinder is symmetric about $x = 0$ the height h_m is attained at two x values, $x = \pm x_m$. From equation (4) we may express h_m in terms of the flux: $h_m = 2Q/(U_1 + U_2)$, *i.e.* if we can measure the flux and the velocities U_1, U_2 are known then we can determine the height where $p_x = 0$. Further, using the quadratic approximation to the roller shape we then know $x_m = \sqrt{2R(h_0 - h_m)}$.

3.1 Isoviscous fluid

We now let $\eta = \eta_0$ be a constant and denote the pressure $p = p_i$, in which case it is relatively simple to integrate (5). With h defined by (2) we find

$$\begin{aligned}\frac{p_i}{6\eta_0(U_1 + U_2)} &= -\frac{x}{8h_0^2 h^2}[3hh_m + 2h_0 h_m - 4h_0 h] \\ &+ \frac{R(4h_0 - 3h_m)}{4h_0^2\sqrt{2h_0 R}} \tan^{-1}\left(\frac{x}{\sqrt{2h_0 R}}\right) + C \,. \end{aligned} \tag{6}$$

We have now determined the form of the pressure, but still need to find the two constants of integration, h_m and C.

Applying $p_i \to 0$ as $x \to -\infty$ (and, since $h \sim x^2$, $h \to \infty$) we find

$$C = \frac{R(4h_0 - 3h_m)}{4h_0^2\sqrt{2h_0R}} \frac{\pi}{2} .$$

Ahead of the nip the pressure reaches zero at a finite point, where the film splits and moves apart on the two rollers, so we impose $p_i(a) = 0$, where $x = a$ is the unknown position of the split. We therefore require a further condition, the cavitation condition $p_{i_x}(a) = 0$ [1], to determine the location of this point. Note, we impose this condition to prevent negative pressures within the film. If the pressure becomes negative it would suck fluid from the split backwards. From our knowledge of the general form of the pressure profile it is apparent that $a = x_m$.

The pressure inside the oil layer may now be written

$$\begin{aligned}\frac{p_i}{6\eta_0(U_1+U_2)} &= -\frac{x}{8h_0^2h^2}[3hh_m + 2h_0h_m - 4h_0h] \\ &+ \frac{R(4h_0 - 3h_m)}{4h_0^2\sqrt{2h_0R}}\left[\tan^{-1}\left(\frac{x}{\sqrt{2h_0R}}\right) + \frac{\pi}{2}\right] . \qquad (7)\end{aligned}$$

Applying $p_i(x_m) = 0$ leads to

$$0 = -\frac{x_m}{8h_0^2h_m}[3h_m - 2h_0] + \frac{R(4h_0 - 3h_m)}{4h_0^2\sqrt{2h_0R}}\left[\tan^{-1}\left(\frac{x_m}{\sqrt{2h_0R}}\right) + \frac{\pi}{2}\right] . \qquad (8)$$

For ease of notation we now set $h_m = \gamma h_0$ where $\gamma > 1$ and hence $x_m = \sqrt{2Rh_0(\gamma-1)}$. Equation (8) may now be reduced to

$$0 = -\sqrt{(\gamma-1)}(3\gamma-2) + \gamma(4-3\gamma)\left[\tan^{-1}\left(\sqrt{\gamma-1}\right) + \frac{\pi}{2}\right] . \qquad (9)$$

This equation determines γ uniquely. It has no dependence on other parameters. The numerical solution gives $\gamma = 1.22575$.

At this stage we still do not know the minimum height h_0. The standard method for determining h_0 is to calculate the load, F, supported by the fluid

$$F = \int_{-\infty}^{x_m} p_i(x)dx . \qquad (10)$$

The load, which represents the weight of the rollers and any external applied force, is a known quantity, hence h_0 may be calculated from this equation.

However, in the current study our aim is to estimate the typical film thickness such that the steel will deform. This gives us an alternative method for calculating h_0.

With the pressure defined by equation (7), the sum of pressures at $\pm x_m$ is

$$\frac{p_i(x_m) + p_i(-x_m)}{6\eta_0(U_1+U_2)} = \frac{R(4-3\gamma)\pi}{4h_0^{3/2}\sqrt{2R}} \,.$$

However, we know that the pressure at the outlet $p_i(x_m) = 0$. Deformation requires the maximum pressure to equal the yield stress σ_Y. We therefore set the maximum pressure $p_i(-x_m) = \sigma_Y$ to give

$$\frac{\sigma_Y}{6\eta_0(U_1+U_2)} = \frac{R(4-3\gamma)\pi}{4h_0^{3/2}\sqrt{2R}} \,,$$

which implies that

$$h_0 = \left(\frac{3R(4-3\gamma)\pi\eta_0(U_1+U_2)}{2\sigma_Y\sqrt{2R}}\right)^{2/3} \,. \tag{11}$$

We now have an expression for the minimum film thickness in terms of the problem parameters. Taking the values $\sigma_Y = 2\times10^8$, $\eta_0 = 0.1$, $U_1+U_2 = 1$, $\gamma = 1.22575$, $R = 0.5$, we find $h_0 \sim 5.25\times10^{-7}$m. This extremely low value is of the order of the surface roughness and indicates that the isoviscous model is not sufficient to describe the problem. We therefore now move on to the piezoviscous model, which the simple argument of the previous section indicated to be necessary.

3.2 Piezoviscous fluid

In this case $\eta = \eta_0 e^{\alpha p}$ and we denote $p = p_v$. Equation (5) becomes

$$e^{-\alpha p_v}\frac{\partial p_v}{\partial x} = \frac{6\eta_0(U_1+U_2)(h-h_m)}{h^3} \,. \tag{12}$$

The integration follows as above and, after applying $p_v \to 0$ as $x \to -\infty$ we obtain

$$\begin{aligned} p_v &= -\frac{1}{\alpha}\ln\left(1 + 6\alpha\eta_0(U_1+U_2)\left\{\frac{x}{8h_0^2h^2}[3hh_m + 2h_0h_m - 4h_0h]\right.\right. \\ &\qquad \left.\left. -\frac{R(4h_0-3h_m)}{4h_0^2\sqrt{2h_0R}}\left[\tan^{-1}\left(\frac{x}{\sqrt{2h_0R}}\right)+\frac{\pi}{2}\right]\right\}\right) \\ &= -\frac{1}{\alpha}\log(1-\alpha p_i) \,. \end{aligned} \tag{13}$$

Applying $p_v(x_m) = 0$ we find

$$\log(1 - \alpha p_i(x_m)) = 0$$

which implies that

$$p_i(x_m) = 0$$

and so γ is again the root of equation (9). Following the same method as in the previous section we find h_0 is defined as:

$$h_0 = \left[\frac{3\alpha\eta_0\pi R\,(U_1 + U_2)\,(4 - 3\gamma)}{2\sqrt{2R}\,(1 - e^{-\alpha\sigma_Y})} \right]^{2/3} \qquad (14)$$

Since x_m depends on h_0, the value of x_m for a piezoviscous model will be different to that obtained from the isoviscous case. With the parameter values of the previous section and $\alpha = 2 \times 10^{-8}$ we find $h_0 \sim 1.34 \times 10^{-6}$m. So, the increase in the fluid viscosity has resulted in an increase in the minimum film thickness by a factor of more than 2.

3.3 Results

Pressure profiles for the isoviscous and piezoviscous cases are shown in Figure 3. The curves correspond to the appropriate limiting minimum thickness, where the maximum pressure equals the yield stress, *i.e.* $h_0 \sim 5 \times 10^{-7}$ for the isoviscous case and $h_0 \sim 1.4 \times 10^{-6}$ for the piezoviscous case. If we choose the same h_0 for each case we will find that the piezoviscous pressure is much higher for the isoviscous one. For example if $h_0 = 1.3 \times 10^{-6}$ the maximum value of p_v is $0.63\sigma_Y$, for p_i the maximum value is $0.23\sigma_Y$. Note, the value of x_m is different in each case, hence the peaks and the ends of the contact occur in different places. Although the roller radius is 0.5m, the actual high pressure region only occurs over about 4mm, justifying the quadratic approximation.

4 Plastic deformation

The purpose of the cold rolling process is to induce plastic deformation within the metal strip and so reduce its thickness. This investigation therefore cannot be complete without an analysis of the plastic deformation.

There exists a significant literature on the cold rolling of steel. Modern studies are primarily numerical, however a good description of early analytical results is given in [4, pp320–328]. Of course the analytical studies require various (sensible) approximations. In particular that:

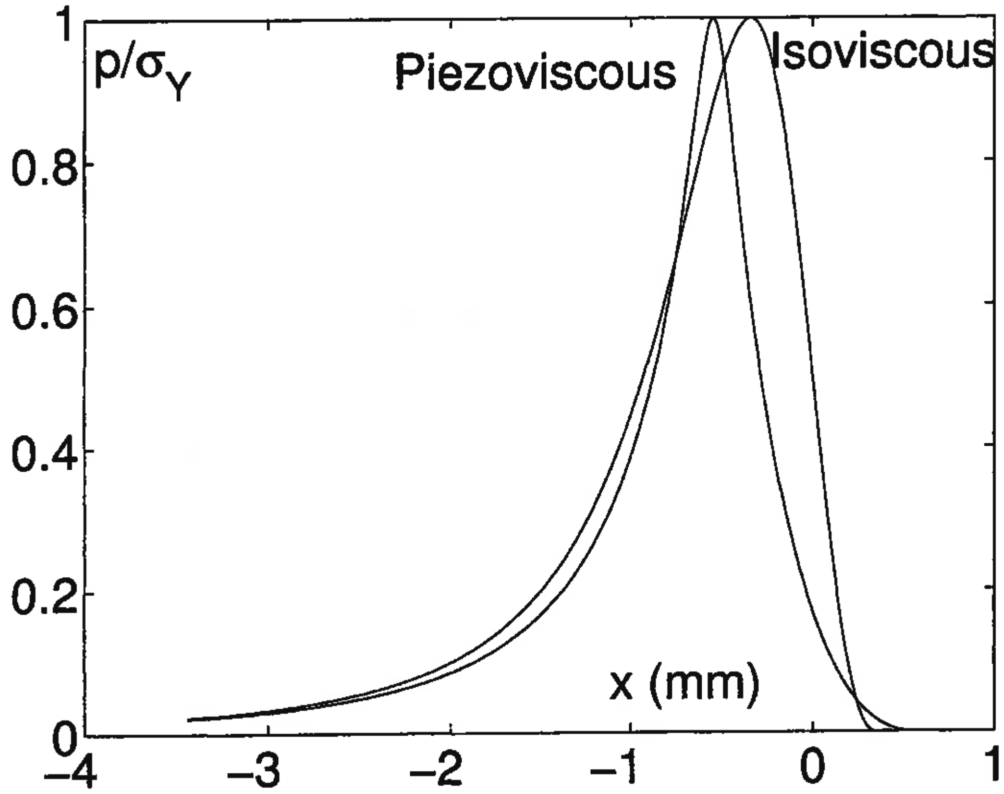

Figure 3: Comparison of isoviscous and piezoviscous pressure profiles

- The elastic deformation of the strip is small compared to the plastic deformation, so that the material is treated as a rigid-plastic.
- The lubricant permits slip everywhere.
- Internal heating due to plastic working of the strip is negligible (this was shown to be the case during the workshop).
- Elastic deformation of the rollers is negligible (this is usually reasonable except for when dealing with very thin, hard strips).
- Lateral deformation is negligible (hence the analysis near the strip edges may be inaccurate).

The onset of plastic flow in the strip depends upon the strip thickness. A thick strip may be approximated as a half-plane which means that plastic deformation occurs when the contact pressure $p = 1.67Y$, where Y is the yield stress of the material in compression. A thinner strip will yield when

$$|\sigma_x - \sigma_z|_{max} = Y \ .$$

For frictionless (or lubricated) materials the shear stress $\sigma_x \ll \sigma_z$ and $\sigma_z = -p$. Yield therefore occurs in a thin strip when $p \approx Y$. This is significantly lower than for a very thick strip. In the following we use this lower bound.

Note that effectively we are neglecting the lubricant except for its effect on the stress σ_x. It's thickness is negligible compared to the strip thickness and so does not enter the plasticity calculation.

Johnson [4] gives a concise description of plastic strip rolling with and without lubricants. The general problem is defined by von Karmans equations, which must be solved numerically. Johnson provides an approximate version with which analytical progress may be made. The simplified version is

$$t\frac{dp}{dx} = 2Y\frac{x}{R} + 2q\,, \tag{15}$$

where the thickness t is taken as the average of $t = (t_i + t_o)/2$. The frictional traction $q = \pm\mu p$ and the coefficient of friction μ is large for hot rolling, for cold rolling it is small (but non-zero, since the fluid exerts a shear force on the roller). Jiang *et al* [3] measure the friction coefficient for a rolling speed of 0.12 m/s and with a reduction of strip thickness around 30%. They find μ varies between 0.3 at the inlet down to zero at the neutral point and rising to 0.1 at the outlet. For simplicity, in the following analysis we will take μ to be constant. The $\pm$ sign denotes whether the stress is positive or negative. This is determined based on the 'neutral point'. At the inlet the strip moves slower than the rollers, at the outlet the strip moves faster, somewhere in between the strip and roller velocities must match. This is the neutral point (although the neutral point may be a neutral region in reality). The problem configuration has already been shown on Figure 1.

If we substitute for q in (15) we find

$$\frac{dp}{dx} \pm 2\mu\frac{p}{t} = 2Y\frac{x}{Rt} \tag{16}$$

where the negative sign holds between the inlet and neutral point, the positive sign holds in the remaining region. The plastic deformation region ends where the roller has a minimum, $x = 0$. We denote the start of the region as $x = -b$. We can then integrate (16) over the two regions. For $x \in [-b, x_n]$ we find

$$p = Y\left[\left(1 + \frac{t - 2\mu b}{2\mu^2 R}\right)e^{2\mu(b+x)/t} - \frac{t + 2\mu x}{2\mu^2 R}\right] \tag{17}$$

where $p(-b) = Y$. For $x \in [x_n, 0]$ we find

$$p = Y\left[\left(1 + \frac{t}{2\mu^2 R}\right)e^{-2\mu x/t} - \frac{t - 2\mu x}{2\mu^2 R}\right]\,, \tag{18}$$

where $p(0) = Y$.

At $x = x_n$ the two pressure expressions must be equal. Equating them determines the position of the neutral point

$$x_n \approx b\left[-\frac{1}{2} + \frac{t}{4\mu^2 R}\left(1 - e^{-\mu a/t}\right)\right] . \tag{19}$$

For a high viscosity fluid or thin strip this will result in $x_n \sim -b/2$. For a lower viscosity fluid, or thicker metal strip the neutral point will move forward, towards the outlet.

The load supported by the film may be determined by integrating the pressure expressions:

$$F = \frac{bY}{2}\left[\frac{t(2\mu^2 bR + bt)}{\mu^3 b^2 R}\left(e^{-2\mu x_n/t} - 1\right) + \frac{b}{\mu R} + \frac{2tx_n}{\mu^2 bR} - \frac{2x_n^2}{\mu bR}\right] . \tag{20}$$

Similarly, the moment exerted by the fluid on the roller is

$$M = \frac{b^2 Y}{2}\left[\frac{t}{2\mu^2 R}\left(1 - 4\frac{x_n^2}{b^2} + 4\frac{x_n t}{2\mu b^2}\right) - \frac{t(2\mu^2 bR + bt)}{\mu^3 b^3 R} x_n e^{-2\mu x_n/t}\right.$$
$$\left. + \frac{2b}{3\mu R}\left(1 + 2\frac{x_n^3}{b^3}\right) - \frac{t}{\mu b}\right] . \tag{21}$$

Provided the moment (or torque) can be measured this final equation should permit us to determine an average value for μ.

In Figure 4 we show two typical pressure profiles in the plastic region. The conditions employed were $a = 2$mm, $R = 0.5$m, $\mu = 1$ and $t = 1$ and 5 cm. This gives $x_n \sim -1$mm $\sim a/2$. A comparison of x_n calculated exactly and using the approximate formula showed an accuracy of greater than 0.1%. Both profiles increase to a maximum at x_n and subsequently decrease. The approximately linear nature of the curves indicates that the exponential terms are small and could be neglected in a more approximate analysis. In both cases the pressure exceeds the yield stress. Recall, in the previous section we limited the fluid pressure to be below the yield stress. Decreasing the strip thickness leads to an increase in the maximum pressure. Outside of the plastic region the hydrodynamic solutions of the previous sections could be patched on, however we would need to recalculate the length of the contact region to do this accurately. We will not carry this out because the change in lengths will simply amount to a small correction, further, as we have shown the viscosity variation will be significant at such high pressures and so to sensibly carry the work forward we should incorporate this effect into the analysis as well.

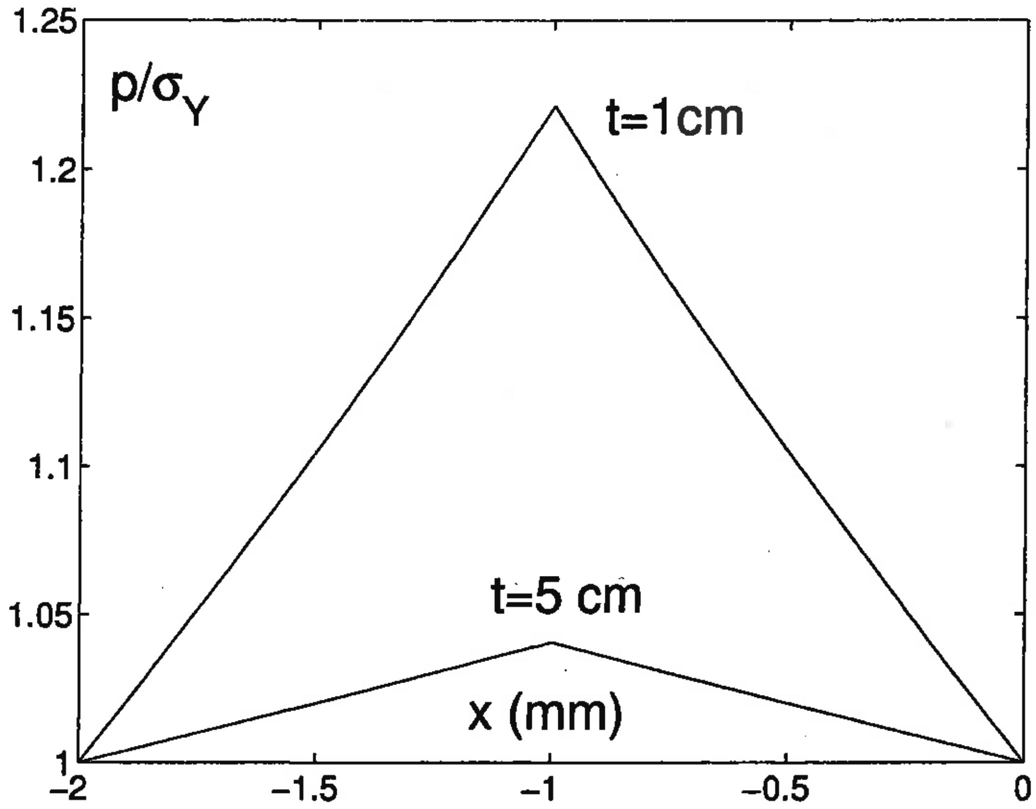

Figure 4: Pressure profile in plastic deformation region for 1 and 5 cm average thickness strips

5 Conclusions and further work

In this report we have developed basic models for the fluid and solid behaviour. First we investigated the lubricant behaviour under conditions typical of cold rolling. This showed that the viscosity is likely to show a significant increase due to the high pressures and a much less significant decrease due to the temperature variation. We then considered isoviscous flow under a rigid roller, which resulted in film thickness predictions below typical surface roughness values. Incorporating the effect of viscosity variation led to film thicknesses approximately twice those of the isoviscous theory. However, this was still on the order of surface roughness scales.

Obviously at some stage we had to introduce plasticity. Following the analysis of Johnson [4] we were able to produce typical pressure profiles within the deformed region. These showed that the pressure can exceed the yield stress, and it increases with decreasing strip thickness. The simple form for the pressure profile (approximately linear) indicates that even greater approximations could be made to further simplify the analysis and hence avoid computation when we introduce other effects, such as combining lubrication with plasticity.

The basic work of this report leaves a lot of avenues unexplored, however it does pave the way for further work. In the future it would clearly be of benefit to incorporate or at least investigate the following:

- **Effect of roughness**

  During the manufacture of the rollers grooves form perpendicular to the axis, with the effect that there is a cross-roller variation in height. At the study group we carried out a preliminary analysis to show the effect of these grooves on the pressure. This should be taken further. Basically this could be done by perturbing the solution given in §3. Adding a periodic variation in the cross roller direction of the form

  $$h = h_0 + \frac{x^2}{2R} + \epsilon e^{i\omega y}$$

  should allow analytical progress and permit us to estimate the effect of the grooves on the fluid pressure.

  Roughness should also be accounted for due to the presence of asperities on the strip. This is dealt with in [5, 7, 10], where asperity crushing is discussed in some detail.

- **Lubricant behaviour**

  So far we have included pressure-viscosity effects, however the viscosity can also be affected by temperature and shear/strain rate. In §2 we showed that pressure was much more important than temperature rise, but the temperature variation can decrease the viscosity by a factor of around 2/3. This will therefore lead to a decrease in the minimum film thickness. The effect of strain rate on viscosity is discussed in [9] (although their calculations all appear to involve only pressure effects).

  It is well known that fluids subject to high strain rates can generate heat internally. During the meeting it was shown both numerically and analytically that in the current situation this would be negligible.

  Given the film heights predicted by our calculations, it appears that we will always be operating with thicknesses close to the asperity height. In which case a 'mixed lubrication' model will be appropriate. This really means that pockets of lubricant are trapped between asperities. The effect on the Reynolds equation (5) has been modelled by simply introducing a flow factor (possibly better termed as a fudge factor) so that $p \to \phi p$, see [6, 8].

- **Combined plasticity-lubrication model**

  The basic plasticity model that we used could be linked in a number of ways to the lubrication analysis. Firstly, it should be simple to link inlet and outlet lubrication zones to the central plasticity zone. Currently the plasticity model stops when the pressure reaches the yield stress, outside this region the pressure is zero. Secondly, the lubricant has been effectively neglected within the plastic region, aside from saying that it reduces friction. The lubrication model could be carried inside the plastic zone.

  There is also scope for a number of experiments to determine parameters that were estimated during this work, for example the 'average viscosity', which requires knowledge of the moment and the length of the plastic zone which comes from the applied load.

Finally, it should be pointed out that this report really only scratches the surface of the problem. A similar problem was investigated at an Australian meeting in 1994 [11], with little progress. Given more time and more resources greater progress could be rapidly made. There is clearly a great deal of analysis and numerics left to be done as well as the extensions mentioned above and presumably other extensions that would crop up through further investigation.

References

[1] Cameron A. Principles of lubrication. Longmans (1966).

[2] Dowson D. and Higginson G.R. Elastohydrodynamic lubrication. Pergamon Press, Oxford (1977).

[3] Jiang Z.Y., Tieu A.K. and Zhang X.M. Finite element modelling of mixed film lubrication in cold strip rolling. *J. Materials Proc. Tech.* **151** (2004), 242-247.

[4] Johnson K.L. Contact Mechanics. Cambridge University Press (1985).

[5] Le H.R. and Sutcliffe M.P.F. Evolution of surface pits on stainless steel strip in cold rolling and strip drawing. *J. Tribology, Trans ASME* **125** (2003), 384-390.

[6] Liu Y.J. and Tieu A.K. A thermal mixed film lubrication model in cold rolling. *J. Materials Proc. Tech.* **130-131** (2002), 202-207.

[7] Lu C., Tieu A.K. and Jiang Z. Modeling of the inlet zone in the mixed lubrication situation of cold strip rolling. *J. Materials Proc. Tech.* **140** (2003), 569-575.

[8] Patir N. and Cheng H.S. Application of average flow model to lubrication between rough sliding surfaces. *J. Lubric. Tech.* **101** (1979), 220-230.

[9] Saxena S., Dixit P.M. and Lal G.K. Analysis of cold strip rolling under hydrodynamic lubrication. *J. Materials Proc. Tech.* **58** (1996), 256-266.

[10] Stephany A., Ponthot J.P., Collette C. and Schelings J. Efficient algorithmic approach for mixed lubrication in cold rolling. *J. Materials Proc. Tech.* **153-154** (2004), 307-313.

[11] A simple model for the cold rolling of metal foil. Proceedings Mathematics in Industry Study Group, Australia (1994).